Molecular and Electronic Structure of the Electron-Transfer Probe Analogue [*trans*-$(NH_3)_4$Ru(imidazole)(isonicotinamide)]-$(CF_3CO_2)_3$·2-propanol

James F. Wishart, Xiaohua Zhang, Stephan S. Isied,* Joseph A. Potenza,* and Harvey J. Schugar*

Department of Chemistry, Rutgers, The State University of New Jersey, New Brunswick, New Jersey 08903

Received October 16, 1991

Kinetic and thermodynamic studies of long-range electron transfer[1] in cytochrome *c*,[2-5] azurin,[6,7] and myoglobin[8] have exploited the modification of these metalloprotein surfaces with ruthenium ammine probes attached to surface histidine imidazole groups. Our combined structural, polarized electronic spectroscopic, and calculational study[9] of the (L-histidinato)$(NH_3)_5Ru^{III}$ chromophore characterized the strong $d\pi/p\pi$ overlap between the Ru(III) d-vacancy and the histidine imidazole π-system. One implication of this study for the use of $(NH_3)_5Ru^{III}$(his) probes as surface electron acceptors is that the effective electron-transfer pathway from the protein active site should be that calculated to the edge of the probe imidazole unit rather than to the metal center. Use of the modified surface probe *trans*-$(NH_3)_4$(isonicotinamide)$Ru^{III/II}$(his) in the cytochrome *c* system results in an approximate reversal of the driving force for electron transfer.[4] This strategy was used to explore the effect of the directionality of electron transfer on the rate of electron transfer in this protein at constant driving force. With the modified probe, electron transfer is observed from the reduced Fe(II) cytochrome to the Ru(III) center whereas the parent pentaammine probe is used to study electron transfer from Ru(II) to the Fe(III) cytochrome center.

The UV–vis spectrum of the Ru(III) center in the covalently bound $Ru^{III}(NH_3)_4$(his)(isonicotinamide) cytochrome *c* system is difficult to determine owing to strong overlapping absorptions from the heme protein. Moreover, the $Ru^{III}(NH_3)_4$(his)-(isonicotinamide) probe (see Results and Discussion) has only limited stability at neutral pH (ca. minutes), making crystallization of the modified protein difficult. Thus, no information has been obtained on the angular relationship between the histidine imidazole and the isonicotinamide groups in $Ru^{III}(NH_3)_4$-(his)(isonicotinamide)-modified cytochrome *c* and its effects on the electronic spectrum of this chromophore. Depending upon the mutual orientations and electronic properties of the isonicotinamide and imidazole rings in the modified probe, coupling of the Ru(III) d-vacancy to the imidazole could be substantially different from that of the parent $(NH_3)_5Ru^{III}$(his) probe and thus might constitute an additional barrier in the electron-transfer pathway. These questions prompted us to examine in detail the structure and electronic spectroscopic properties of *trans*-$(NH_3)_4$-Ru^{III}(isonicotinamide)(imidazole).

Experimental Section

1. Preparation of the Title Complex 1. [*trans*-$(NH_3)_4$Ru(imidazole)-(isonicotinamide)]$(ClO_4)_2$ (**2**), was prepared by reducing a solution of *trans*-[$(NH_3)_4Ru(SO_4)$(isonicotinamide)]Cl[10] (220 mg, 0.52 mmol) and imidazole (140 mg, 2.1 mmol) in 3 mL of water with zinc amalgam under argon for 90 min. The solution was transferred to a flask containing 3 mL of saturated, argon-degassed $NaClO_4$ solution, and a fine precipitate of dark, iridescent crystals formed. After 15 min, the solid was collected by filtration, washed with ethanol, 1:4 v/v ethanol/ethyl ether, and ether, and dried in vacuo overnight (yield 240 mg, 83%).

Complex **1** was prepared by oxidation of **2** (118 mg, 0.21 mmol) with silver trifluoroacetate (51.4 mg, 0.23 mmol) in 10 mL of water. The solution turned from deep to pale orange, and silver metal precipitated. The solution was filtered through a 0.4-μm membrane filter and applied to a column of Sephadex SP-25 ion-exchange resin that had been pretreated with alkaline hydrogen peroxide and neutralized before use. A single band which eluted with a gradient between 0.3 and 1.0 M trifluoroacetic acid was concentrated to dryness by rotary evaporation. The residue was dissolved in ca. 7 mL of ethanol, precipitated by slow addition of 20 mL of ethyl ether, filtered off, washed with ether, and dried in vacuo overnight to give 102 mg (ca. 15% yield) of an orange solid. Crystals of **1** suitable for X-ray diffraction were grown by vapor diffusion of methanol into a saturated solution of the orange solid in 2-propanol.

2. Physical Measurements. Reduction potentials of the complexes were determined by cyclic voltammetry using a three-electrode configuration (platinum disk working electrode, SCE reference electrode, platinum wire auxiliary electrode) with a BAS 100 instrument (Bioanalytical Systems, West Lafayette, IN). Electronic spectra were recorded using a Hewelett Packard 8452 diode array spectrophotometer and a Cary 14 spectrophotometer modified by Aviv Associates.

3. X-ray Diffraction Studies. A crystal of **1** was mounted inside a glass capillary that contained a small amount of mother liquor well removed from the crystal. Diffraction measurements were made on an Enraf-Nonius CAD-4 diffractometer. The Enraf-Nonius Structure Determination Package[11] was used for data collection, processing, and structure solution. Crystal data are presented in Table I. Three standard reflections showed a decrease of 20.0% over the period of data collection, despite the precautions taken to avoid loss of solvate. Intensity data were corrected for decay, absorption (empirical, ψ-scan), and LP effects.

The structure was solved by direct methods[12] and refined on *F* with full-matrix least-squares techniques. An initial *E* map and successive difference Fourier maps revealed the coordinates of the non-hydrogen atoms. One of the CF_3 groups was found to exhibit a positional disorder. On the basis of electron density, this group was modeled with six F atoms, each with an occupancy factor of 0.5. Following refinement of the heavy atoms, several H atoms were located on a difference map. Coordinates for the remaining H atoms were calculated by assuming idealized bond geometries and respective C–H and N–H distances of 0.95 and 0.87 Å, except for those of the 2-propanol solvate methyl groups, which were not included in the structure. H atom parameters were not refined. Anisotropic refinement converged with $R_F = 0.050$, $R_{wF} = 0.057$, and GOF = 1.70. Thermal parameters for the F atoms of the anion CF_3 groups and the solvate CH_3 groups were substantially larger than those of the remaining atoms. Atomic parameters for the cation atoms are listed in Table II, while a view of the cation is shown in Figure 1. Additional crystal and refinement data and complete lists of coordinates, anisotropic thermal parameters, bond distances and angles for the anion and solvate species, and observed and calculated structure factors are available.[13]

Results and Discussion

1. Crystal Structure. The structure contains approximately octahedral *trans*-[$(NH_3)_4$Ru(isonicotinamide)(imidazole)]$^{3+}$ cat-

(1) (a) Mayo, S. L.; Ellis, W. R., Jr.; Crutchley, R. J.; Gray, H. B. *Science* **1986**, *233*, 948–52. (b) Isied, S. S. In *Metal Ions in Biological Systems*; Sigel, H., Sigel, A., Eds.; Marcel Dekker, Inc.: New York, 1991; Vol. 27, pp 1–56.
(2) Nocera, D. G.; Winkler, J. R.; Yocom, K. M.; Bordignon, E.; Gray, H. B. *J. Am. Chem. Soc.* **1984**, *106*, 5145–50.
(3) Isied, S. S.; Kuehn, C.; Worosila, G. *J. Am. Chem. Soc.* **1984**, *106*, 1722–6.
(4) Bechtold, R.; Kuehn, C.; Lepre, C.; Isied, S. S. *Nature (London)* **1986**, *322*, 286–8.
(5) Therien, M. J.; Selman, M.; Gray, H. B.; Chang, I.-J.; Winkler, J. R. *J. Am. Chem. Soc.* **1990**, *112*, 2420–2.
(6) Margalit, R.; Kostic, N. M.; Che, C.-M.; Blair, D. F.; Chiang, H.-J.; Pecht, I.; Shelton, J. B.; Shelton, J. R.; Schroeder, W. A.; Gray, H. B. *Proc. Natl. Acad. Sci. U.S.A.* **1984**, *81*, 6554–8.
(7) Gray, H. B. *Chem. Soc. Rev.* **1986**, *15*, 17–30.
(8) Crutchley, R. J.; Ellis, W. R., Jr.; Gray, H. B. *J. Am. Chem. Soc.* **1985**, *107*, 5002–4.
(9) Krogh-Jespersen, K.; Westbrook, J. D.; Potenza, J. A.; Schugar, H. J. *J. Am. Chem. Soc.* **1987**, *109*, 7025–31.
(10) Isied, S. S.; Taube, H. *Inorg. Chem.* **1976**, *15*, 3070–5.
(11) Enraf-Nonius Structure Determination Package, Enraf-Nonius, Delft, Holland, 1985.
(12) Main, P.; Fiske, S. J.; Hull, S. E.; Lessinger, L.; Germain, G.; Declercq, J.-P.; Woolfson, M. M. MULTAN 82: A System of Computer Programs for the Automatic Solution of Crystal Structures from X-ray Diffraction Data. Universities of York, England, and Louvain, Belgium, 1982.
(13) Supplementary material.

0020-1669/92/1331-3179$03.00/0 © 1992 American Chemical Society

Table I. Crystal Data for **1**[a]

formula	$RuF_9O_8N_8C_{18}H_{30}$	fw	758.54
space group	$P\bar{1}$	Z	2
cryst syst	triclinic	D_c, g/cm^3	1.671
a, Å	12.259 (3)	temp, °C	23 (1)
b, Å	13.367 (3)	radiation (λ, Å)	Mo (0.710 73)
c, Å	10.175 (2)	2θ range, deg	4–44
α, deg	98.76 (3)	no. of unique data	3680
β, deg	95.94 (3)	no. of obsd data (3σ)	2593
γ, deg	66.31 (2)	R_F	0.050
V, Å^3	1507.4 (9)	R_{wF}	0.057
μ, cm^{-1}	6.1		

[a] $R_F = \Sigma(|F_o| - |F_c|)/\Sigma|F_o|$. $R_{wF} = [\Sigma w(|F_o| - |F_c|)^2/\Sigma w|F_o|^2]^{1/2}$.

Table II. Atomic Parameters for the Cation in **1**

	x	y	z	B_{eq},[a] Å^2
Ru	0.32795 (6)	−0.17325 (5)	−0.00397 (7)	2.08 (1)
N(1)	0.4228 (5)	−0.1934 (5)	−0.1673 (6)	2.4 (1)
N(2)	0.2348 (5)	−0.1563 (5)	0.1643 (6)	2.5 (2)
N(3)	0.4866 (5)	−0.2809 (5)	0.0869 (6)	3.3 (2)
N(4)	0.3659 (5)	−0.0352 (5)	0.0721 (6)	2.7 (2)
N(5)	0.1724 (5)	−0.0635 (5)	−0.0921 (6)	2.8 (2)
N(6)	0.2848 (6)	−0.3074 (5)	−0.0845 (7)	3.5 (2)
C(1)	0.1286 (6)	−0.1668 (7)	0.1538 (8)	3.4 (2)
C(2)	0.0680 (6)	−0.1607 (7)	0.2627 (8)	3.1 (2)
C(3)	0.1165 (6)	−0.1439 (6)	0.3898 (8)	2.7 (2)
C(4)	0.2232 (6)	−0.1314 (6)	0.4024 (8)	2.8 (2)
C(5)	0.2802 (6)	−0.1387 (6)	0.2890 (8)	2.9 (2)
C(6)	0.5315 (7)	−0.1853 (6)	−0.1684 (8)	3.3 (2)
C(7)	0.5685 (7)	−0.2108 (7)	−0.2923 (8)	3.7 (2)
N(7)	0.4833 (6)	−0.2366 (5)	−0.3714 (6)	3.4 (2)
C(8)	0.3976 (6)	−0.2238 (6)	−0.2912 (8)	2.9 (2)
C(9)	0.0565 (7)	−0.1395 (6)	0.5154 (8)	3.1 (2)
O(1)	0.1158 (5)	−0.1483 (5)	0.6222 (5)	4.5 (2)
N(8)	−0.0569 (5)	−0.1238 (6)	0.5019 (6)	3.5 (2)

[a] Anisotropically refined atoms are given in the form of the isotropic equivalent displacement parameter defined as $(4/3)[a^2B(1,1) + b^2B(2,2) + c^2B(3,3) + ab(\cos\gamma)B(1,2) + ac(\cos\beta)B(1,3) + bc(\cos\alpha)B(2,3)]$.

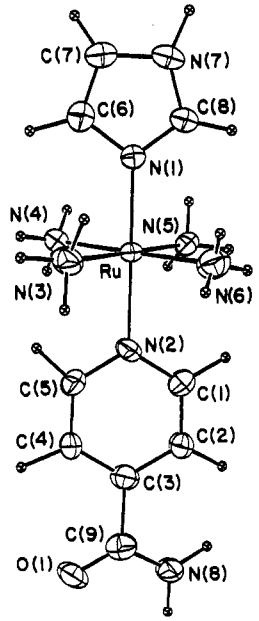

Figure 1. ORTEP drawing of the cation in **1** showing the atom-numbering scheme. Thermal ellipsoids are shown at the 50% probability level. H atoms were located as described in the text.

ions separated by trifluoroacetate anions and 2-propanol solvate molecules. The Ru–N(NH_3) distances span the range 2.095 (7)–2.120 (7) Å with an average of 2.102 (11) Å. This average compares well with those of 2.104 (4) and 2.106 (2) Å reported respectively for $[Ru(NH_3)_6](BF_4)_3$[14] and $[(NH_3)_5RuCl]Cl_2$.[15]

(14) Stynes, H. C.; Ibers, J. A. *Inorg. Chem.* **1971**, *10*, 2304–8.
(15) John, E.; Schugar, H. J.; Potenza, J. A. *Acta Crystallogr.*, in press.

Table III. Selected Bond Distances (Å), Angles (deg), and Torsion Angles (deg) for the Cation in **1**

Ru–N(1)	2.049 (7)	C(1)–C(2)	1.37 (1)
Ru–N(2)	2.090 (6)	C(2)–C(3)	1.39 (1)
Ru–N(3)	2.120 (7)	C(3)–C(4)	1.37 (1)
Ru–N(4)	2.098 (7)	C(3)–C(9)	1.52 (1)
Ru–N(5)	2.095 (7)	C(4)–C(5)	1.38 (1)
Ru–N(6)	2.096 (7)	C(6)–C(7)	1.33 (1)
N(1)–C(6)	1.38 (1)	C(7)–N(7)	1.38 (1)
N(1)–C(8)	1.31 (1)	N(7)–C(8)	1.34 (1)
N(2)–C(1)	1.36 (1)	C(9)–O(1)	1.24 (1)
N(2)–C(5)	1.36 (1)	C(9)–N(8)	1.31 (1)
N(1)–Ru–N(2)	178.5 (3)	Ru–N(2)–C(1)	121.4 (6)
N(1)–Ru–N(3)	88.3 (3)	Ru–N(2)–C(5)	121.4 (5)
N(1)–Ru–N(4)	89.3 (3)	C(1)–N(2)–C(5)	117.2 (7)
N(1)–Ru–N(5)	91.6 (3)	N(2)–C(1)–C(2)	122.6 (8)
N(1)–Ru–N(6)	90.4 (3)	C(1)–C(2)–C(3)	119.5 (8)
N(2)–Ru–N(3)	90.2 (3)	C(2)–C(3)–C(4)	118.7 (8)
N(2)–Ru–N(4)	91.2 (3)	C(2)–C(3)–C(9)	122.6 (8)
N(2)–Ru–N(5)	89.9 (3)	C(4)–C(3)–C(9)	118.7 (8)
N(2)–Ru–N(6)	89.2 (3)	C(3)–C(4)–C(5)	119.1 (8)
N(3)–Ru–N(4)	92.0 (3)	N(2)–C(5)–C(4)	122.9 (7)
N(3)–Ru–N(5)	178.6 (3)	N(1)–C(6)–C(7)	109.5 (8)
N(3)–Ru–N(6)	90.2 (3)	C(6)–C(7)–N(7)	106.9 (8)
N(4)–Ru–N(5)	86.6 (3)	C(7)–N(7)–C(8)	106.4 (7)
N(4)–Ru–N(6)	177.8 (3)	N(1)–C(8)–N(7)	111.8 (8)
N(5)–Ru–N(6)	91.3 (3)	C(3)–C(9)–O(1)	118.5 (8)
Ru–N(1)–C(6)	127.0 (6)	C(3)–C(9)–N(8)	116.7 (8)
Ru–N(1)–C(8)	127.5 (6)	O(1)–C(9)–N(8)	124.8 (8)
C(6)–N(1)–C(8)	105.4 (7)		
N(3)–Ru–N(1)–C(6)	−48.6 (6)	N(3)–Ru–N(2)–C(5)	45.5 (6)
N(4)–Ru–N(1)–C(6)	43.4 (6)	N(4)–Ru–N(2)–C(5)	−46.5 (6)
N(5)–Ru–N(1)–C(8)	−55.0 (6)	N(5)–Ru–N(2)–C(1)	49.5 (6)
N(6)–Ru–N(1)–C(8)	36.3 (6)	N(6)–Ru–N(2)–C(1)	−41.7 (6)

The Ru–N(imidazole) distance, 2.049 (7) Å, is longer than that reported for $(NH_3)_5Ru$(L-histidinato) (2.020 (8) Å)[9] but still shorter than those reported for $(NH_3)_5Ru^{III}$ ligated by pyrazine (2.076 (8) Å),[16] *N*-methylpyrazinium (2.08 (1) Å),[17] hypoxanthine-*N*(7) (2.087 (9) Å),[18] and 7-methylhypoxanthine-*N*(9) (2.094 (6) Å).[18] The Ru–N(isonicotinamide) distance (2.090 (6) Å) compares well with the values of 2.105 (4) and 2.093 (4) Å reported for $[cis\text{-}(NH_3)_4(isonicotinamide)_2Ru](ClO_4)_3\cdot H_2O$.[19] These comparative distances suggest that if there is a structural trans effect between the isonicotinamide and imidazole ligands, it is small at best.

The imidazole ring is essentially planar and oriented such that it bisects approximately the N(3)–Ru–N(4) and N(5)–Ru–N(6) bond angles (see torsion angles, Table III). This result shows that the imidazole ring is staggered with respect to the four "equatorial" NH_3 ligands. A similar orientation exists for the pyridine ring of the isonicotinamide ligand, with the result that both aromatic rings are approximately coplanar (imidazole/pyridine dihedral angle = 8.5 (4)°). Thermal parameters for the anion and solvate species are significantly larger than those for the cation, suggesting that these species are more loosely held in the lattice.

2. Spectroscopy and Electrochemistry. Absorption bands exhibited by **1** in acidic and basic aqueous solution are summarized in Table IV along with that of the corresponding Ru(II) complex. The electronic structures of $(NH_3)_5Ru^{III}$(imidazole) and $(NH_3)_5Ru^{III}$(imidazolate) chromophores have been described

(16) Gress, M. E.; Creutz, C.; Quicksall, C. O. *Inorg. Chem.* **1981**, *20*, 1522–8.
(17) Wishart, J. F.; Bino, A.; Taube, H. *Inorg. Chem.* **1986**, *25*, 3318–21.
(18) Kastner, M. E.; Coffey, K. F.; Clarke, M. J.; Edmonds, S. E.; Eriks, K. *J. Am. Chem. Soc.* **1981**, *103*, 5747–52.
(19) Richardson, D. E.; Walker, D. D.; Sutton, J. E.; Hodgson, K. O.; Taube, H. *Inorg. Chem.* **1979**, *18*, 2216–21.

Table IV. UV–Vis Spectral Data and Assignments

complex	λ_{max}, nm	ϵ	assgnt
[*trans*-$(NH_3)_4Ru^{II}$(imidazole)(isn)]$^{2+}$ [a]	486	6.5×10^3	MLCT
	259	5.2×10^3	$\pi_{isn} \rightarrow \pi^*_{isn}$
[*trans*-$(NH_3)_4Ru^{III}$(imidazole)(isn)]$^{3+}$ [b]	474	3.7×10^2	$\pi_1 \rightarrow$ Ru(III)
	311	4.5×10^3	$\pi_2 \rightarrow$ Ru(III)
	272	6.1×10^3	$\pi_{isn} \rightarrow \pi^*_{isn}$
[*trans*-$(NH_3)_4Ru^{II}$(imidazolate)(isn)]$^{2+}$ [c]	~600	3.7×10^2	$\pi_1 \rightarrow$ Ru(III)
	387	3.3×10^3	$\pi_2 \rightarrow$ Ru(III)
	273	5.8×10^3	$\pi_{isn} \rightarrow \pi^*_{isn}$

[a] Spectra taken in water; isn = isonicotinamide. [b] Spectra taken at pH 1.0, 0.1 M HCl. [c] Spectra taken under Ar at 5 °C, 10 s after raising the pH to 9.9 with carbonate/bicarbonate buffer.

elsewhere.[9,20] Such chromophores show two low-energy imidazole(ate) → Ru(III) charge-transfer (CT) bands which originate from the HOMO (π_1) and SHOMO (π_2) ring π-orbitals having respectively small and moderate coefficients at the nitrogen donor group to which the Ru(III) is bound. The CT band from the SHOMO was observed to be 7–13 times more intense than that from the HOMO. Moreover, the observed energy difference (ca. 9000 cm^{-1}) between these CT bands approximates the energy difference between π_1 and π_2 in the free ligands. Deprotonation of the imidazole ligands to afford imidazolates raises the energies of both the HOMO and SHOMO, with the result that both CT bands are red-shifted by ca. 5000 cm^{-1} while maintaining the same relative intensities and energy differences.

The electronic spectra of **1** in acidic aqueous solution includes low-energy absorptions at 474 and 311 nm whose intensities, energy differences, and red shifts in alkaline solution to ca. 600 and 387 nm, respectively, are consistent with assignment as π_1, $\pi_2 \rightarrow$ Ru(III) CT absorptions. The higher energy band of **1** at 272 nm corresponds to the expected localized $\pi \rightarrow \pi^*$ transition of the isonicotinamide ligand and is displayed at the same energy by the reference $[(NH_3)_5Ru$(isonicotinamide)$]^{3+}$ complex.[21] The local electronic structure of the Ru^{III}(imidazole) unit is not greatly perturbed by the substitution of a trans isonicotinamide ligand for a trans ammine ligand, in harmony with the at best small structural trans effect noted above. Similarly, the local electronic structure of the precursor Ru^{II}(isonicotinamide) unit appears little perturbed by the presence of the trans imidazole ligand. The metal → ligand CT band at 486 nm of this reduced precursor of **1** (Table IV) has an energy and an intensity close to those reported for the reference $[(NH_3)_5Ru$(isonicotinamide)$]^{2+}$ complex.[21]

The reduction potential of **1** was found to be +0.165 V vs SCE (+0.407 V vs NHE, ΔE_{peak} = 61 mV) by cyclic voltammetry in 0.1 M NaCl. This value is slightly lower than that reported for the reference ion $[(NH_3)_5Ru$(isonicotinamide)$]^{3+}$ (0.44 V vs NHE),[21] indicating that the large preferential stabilization of the Ru(II) valence state by the π-acceptor isonicotinamide ligand is not changed appreciably by a trans imidazole group. In basic media (pH 9.9), **1** is unstable and appears to disproportionate to the corresponding Ru(II) and Ru(IV) species.[22] Reducing spectral measurement times to a few seconds essentially eliminates spectroscopic interferences from these decomposition products.

(20) Krogh-Jespersen, K.; Schugar, H. J. *Inorg. Chem.* **1984**, *23*, 4390–3.
(21) Gaunder, R. G.; Taube, H. *Inorg. Chem.* **1970**, *9*, 2627–39.
(22) Sun, J.; Isied, S. S. Unpublished results.

The calculational and single-crystal electronic spectral study of the [(L-histidinato)$(NH_3)_5Ru^{III}]^{3+}$ complex showed that its orange color arises from the $\pi_1 \rightarrow$ Ru(III) LMCT band, which is strongly polarized along the Ru(III)–N(imidazole) bond direction; the Ru(III) d-vacancy was oriented for maximal π-bonding with the histidine imidazole group, as in **3**.[9] The orange

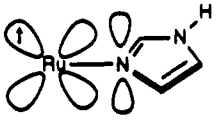

3

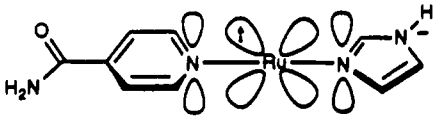

4

color of **1** both in the solid state and in solution has the same origin. These spectroscopic observations along with the structural results for **1** suggest that the Ru(III) d-vacancy is oriented for π-bonding with both the imidazole group and the coplanar trans isonicotinamide ligand, as in **4**. Perhaps there is some cooperative interaction with the weakly π-donating[9] imidazole and the π-accepting isonicotinamide. The situation, **5**, whereby the isonicotinamide and imidazole rings are perpendicular rather than parallel and the d-vacancy is π-bonded only to the former was not observed. Electronic coupling of Ru(III) to the imidazole π-system does not appear to be appreciably reduced by the presence of the trans isonicotinamide ligand. We conclude that the isonicotinamide-modified surface probe does not present any additional electronic barrier to electron transfer over that present in the parent $(NH_3)_5Ru$(histidine) probe.

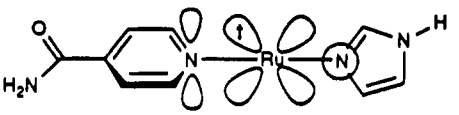

5

3. Conclusion. The difficulty of obtaining electronic–structural information about the Ru center in $Ru^{III}(NH_3)_4$(his)(isonicotinamide)-modified cytochrome *c* prompted a study of the corresponding protein-free Ru(III) chromophore. Owing to the coplanarity of the imidazole and isonicotinamide rings, the electronic coupling between Ru(III) and the imidazole ring, as measured by the features of the imidazole → Ru(III) LMCT absorption, is only minimally changed by replacing a trans NH_3 ligand by isonicotinamide. Barring any unusual structural effects caused by protein–probe interactions, the oxidation and reduction of cytochrome *c* by these covalently attached Ru probe molecules should not be complicated by electronic coupling differences of the type considered above.

Acknowledgment. The research of H.J.S. and J.A.P. was supported by NIH Grant GM-37994, the Charles and Johanna Busch Foundation, and NIH Grant 1510RRO 1486 O1A1 (for the X-ray diffractometer). The research of S.S.I. was supported by the NSF (Grant CHE 8405522) and the Office of Basic Research, Division of Chemical Sciences, U.S. Department of Energy (Grant DE-FG05-90ER1U120).

Supplementary Material Available: Listings of crystal structure data, anion, solvate, and H atom parameters, anisotropic thermal parameters, and additional bond distances and angles and a diagram showing the connectivity of the anion and solvate species (7 pages); a listing of observed and calculated structure factors (15 pages). Ordering information is given on any current masthead page.